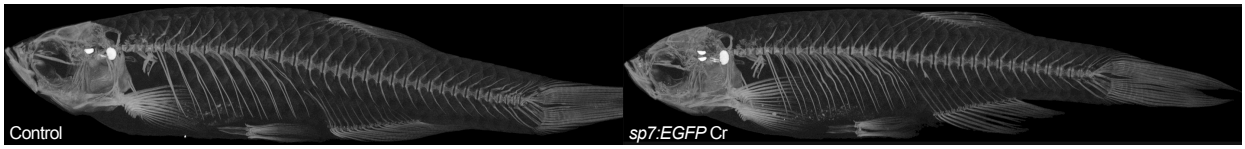

Figure S1, Related to Figure 1. μCT scans of *sp7:EGFP* somatic mutant zebrafish show normal bone morphology. Loss-of-fluorescence does not appear to be attributable to loss of bony tissue as *sp7:EGFP* somatic mutants (right) have grossly normal skeletons as adults.

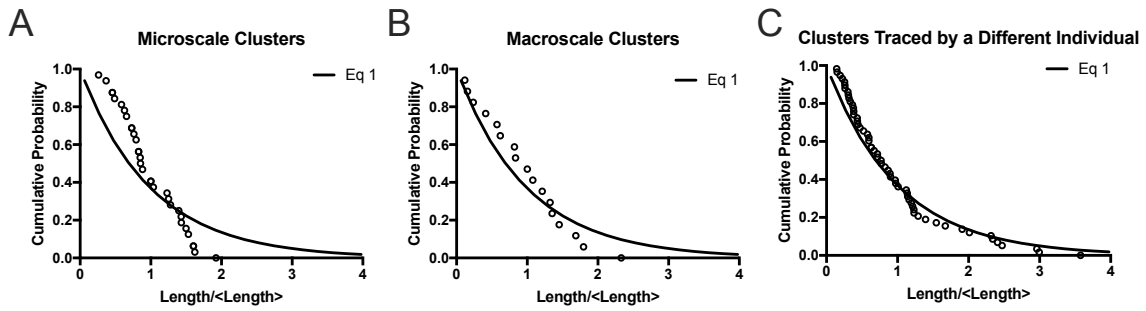

Figure S2, Related to Figure 1. Loss-of-function cluster size distributions are best modeled by fragmentation and merger theory when microscale and macroscale clusters are considered in combination. (A-B) Vertebral cluster size distributions normalized by mean cluster length when microscale (A) and macroscale (B) clusters are treated independently. Note that the curve fit for panels A and B is weaker than that in Figure 1K. (C) The same images used for cluster size analysis in Figure 1K were analyzed by a different individual. Cluster size distributions appear to be robust to thresholding differences between observers.

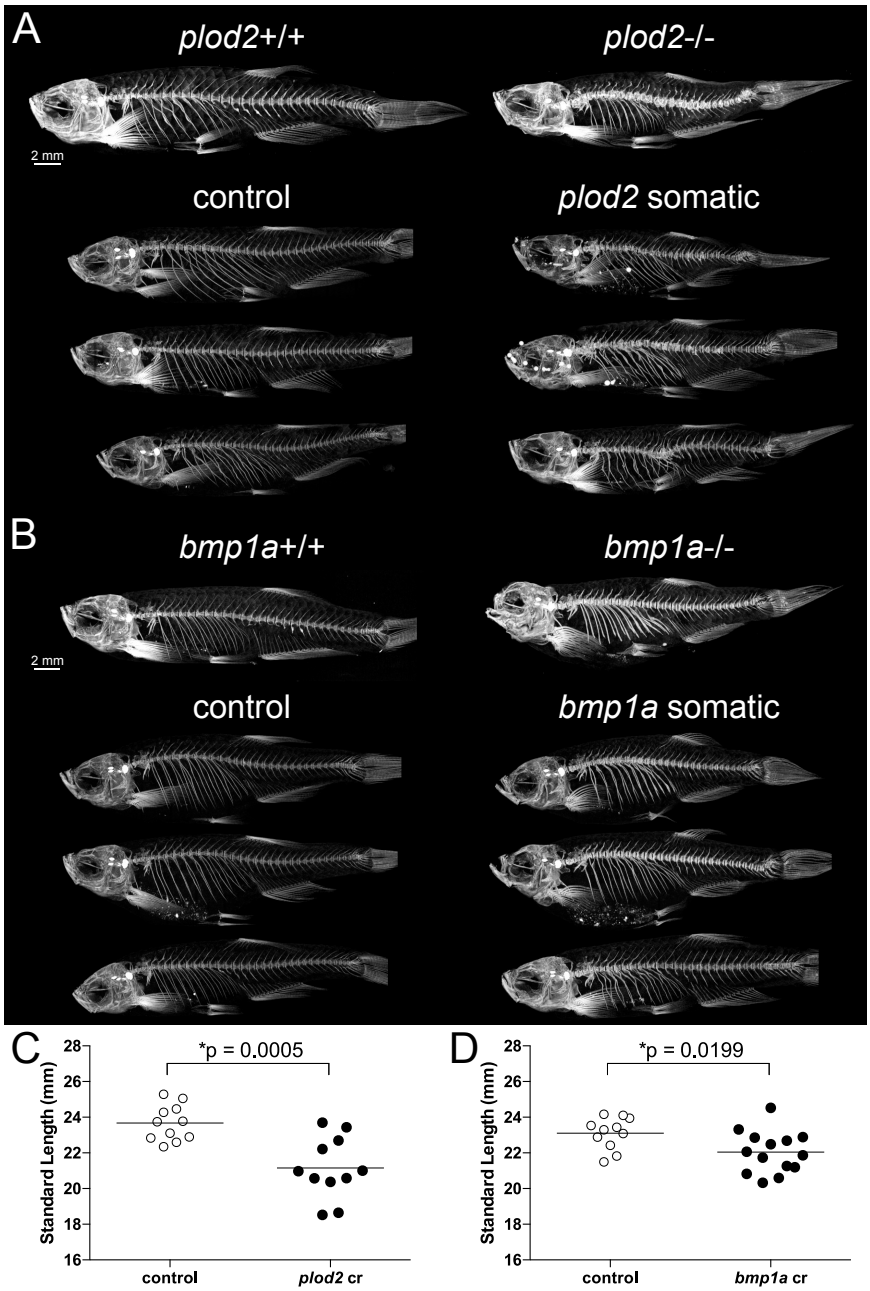

Figure S3, Related to Figure 2. Somatic mutants for *bmp1a* and *plod2* exhibit inter- and intra-animal phenotypic variability. (A-B) Representative maximum intensity projections of microCT scans. Germline controls (+/+) and mutants (-/-) for each gene are shown above somatic cohorts. (A) Irregular expressivity seen in the spine of *plod2* somatic mutants was not evident in the *plod2* germline mutant. (B) Inter-animal variation in radiopacity of the spine for somatic *bmp1a* fish was evident, while intra-animal variation along the axial skeleton was less apparent. (C-D) Somatic mutants are shorter than clutchmates. Standard lengths are statistically reduced in both

somatic lines for *plod2* (C, n=11/group) and *bmp1a* (D, n=11 controls, n=14 *bmp1a* somatic mutants) compared to clutchmate controls.

Figure S4, Related to Figure 2. FishCuT analysis of *plod2* somatic mutants for all 25 combinatorial measures. Phenotypic features, indicated by the graph heading (with units for y-axis), plotted as a function of vertebra (mean ± SE, n = 11/group). Plots associated with $p<0.05$ in the global test are colored in a lighter coloring scheme and denoted by an asterisk in the graph heading. In addition to the 7 of 10 measures plotted in Figure 2B-K (bold titles) that are statistically different, 10 of the remaining 15 measures are also statistically different, including increased variability in tissue mineral density of all structures for *plod2* somatic mutants. Cent, centrum; Haem, haemal arch; Neur, neural arch; Vert, total vertebra; Vol, volume; SA, surface area; Th, thickness; TMD, tissue mineral density; Le, length; sd, standard deviation (variability).

Figure S5, Related to Figure 2. FishCuT analysis of *bmp1a* somatic mutants for all 25 combinatorial measures. Phenotypic features, indicated by the graph heading (with units for y-axis), plotted as a function of vertebra (mean ± SE, n = 15/group). Plots associated with $p<0.05$ in the global test are colored in a lighter coloring scheme and denoted by an asterisk in the graph heading. In addition to the 7 of 10 measures plotted in Figure 2B'-K' (bold titles) that are statistically different, 11 of the remaining 15 measures are also statistically different, including increased variability in tissue mineral density of all structures for *bmp1a* somatic mutants. Cent, centrum; Haem, haemal arch; Neur, neural arch; Vert, total vertebra; Vol, volume; SA, surface area; Th, thickness; TMD, tissue mineral density; Le, length; sd, standard deviation (variability).

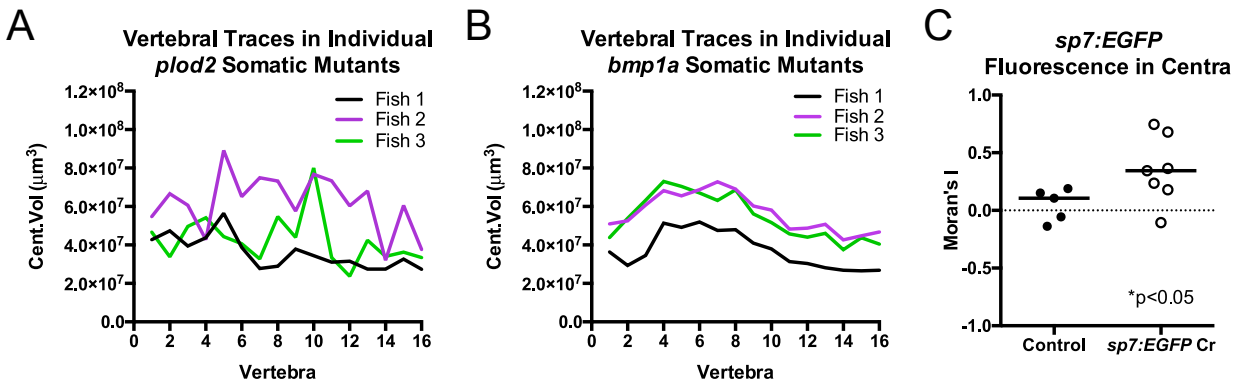

Figure S6, Related to Figures 2 and 4. Vertebral traces for *plod2* and *bmp1a* show inter- and intra-individual variation among somatic groups. (A,B) Vertebral traces for centrum volume of representative *plod2* (A) and *bmp1a* (B) somatic mutants. Traces for *plod2* somatic mutants are jagged (i.e. a high degree of intra-individual variation), whereas those for *bmp1a* somatic mutants appear relatively smooth. Both somatic mutants groups exhibit variability in expressivity across individuals (i.e. inter-individual variation). (C) Intra-individual variation is represented by a shift to a lower distribution of values for Moran's I for *plod2* (see Figure 4G) but not for *bmp1a* (see Figure 4G'). In contrast, Moran's I in *sp7:EGFP* somatic mutant larvae shows a shift towards clustered mosaicism in the centra of these fish. $p<0.05$ in a M.-W. test.

Age (dpf)	Approximate Body Weight (g)	Food Type	% of body weight to feed	Feedings per day	Total amount per day per fish (mg)	Amount per fish per feeding (mg)
11-14	0.01	GM 75	20%	3	1.98	0.66
15-17	0.02	GM 75	20%	3	3.9	1.3
18-23	0.02	GM 150	20%	3	3.9	1.3
24-30	0.04	GM 150	13%	3	5.1	1.7
31-42	0.07	GM 300	10%	2	7	3.5
43-55	0.22	GM 300	7%	2	15	7.5
56+	0.4	GM 300	3%	1	12	12

Table S1, Related to STAR Methods: Experimental Model and Subject Details (*Zebrafish rearing*). Feeding schedule used for experimental fish in the study. Feedings were done on a per fish basis to maintain consistent growth in mutant and control populations.